Document Title:

SEASAT SAR IPF
SEASAT Data and Processing Issues

Technical Note

VEGA Contract : VEGA/AG/08/00705

Prepared by: A.M.Smith
Phoenix Systems

Reference: C-2014-02-01-TN-01
Issue: 1
Revision: 3
Date of issue: May 2014
Status: Issued
Document type: Technical Note
Distribution:

Authorisation

Authorised by: A.M.Smith
Title: Director

Signature: 

Date: 14th May 2014

Record of Changes

Issue	Date	Change Log
1.1	30th April 2014	Creation.
1.2	6th May 2014	Minor editorial and typographic corrections
1.3	14th May 2014	Minor updates to acronyms following review

Table of Contents

Table of Figures

1 Introduction

1.1 Background and Purpose

This document has been prepared for ESA under VEGA contract **VEGA/AG/08/00705 IDEAS Phase 6** relating to the rehabilitation and reprocessing of ESA's historic SEASAT raw data archive.

The purpose of the document is to provide a summary of technical details and issues of potential interest to data users of the reprocessed archive.

1.2 Scope and Document Overview

The primary focus of the document is descriptive; it describes issues and processes but avoids low-level technical discussions and is intended to be readily accessible to a wide audience.

The document contains 3 principal sections:

- Section 2 provides a brief description of the SEASAT mission and the motivation for rehabilitating and reprocessing the archive.
- Section 3 discusses the rationale for and processes undertaken in rehabilitating the raw data archive
- Section 4 summarises the various technical issues and problems associated with this historic dataset and discusses how these have been addressed.

1.3 Reference Documents

[RD-01] Fu & Holt "Seasat Views Oceans and Sea Ice with Synthetic Aperture Radar", Jet Propulsion laboratory, February 15th 1982.

[RD-02] https://www.asf.alaska.edu/seasat/product-specification-guide

[RD-03] Jordon, R "The SEASAT-A Synthetic Aperture Radar System", 0364-9059/80/0400-0154 IEEE 1980

[RD-04] "An Introduction to the Interim Digital SAR Processor and the Characteristics of the Associated SEASAT SAR Imagery", JPL, April 1st 1981

[RD-05] RS EO ESRIN 2010-55 Seasat 1 SAR Spec (EARTHNET)

[RD-06] JERS-1/SEASAT Product Specification JSIPF-PRODUCT-SPEC.v.1.0 April 2014

1.4 Acronyms and Abbreviations

Acronym	*Description*
ADC	Analog to Digital Conversion
AGC	Automatic Gain Control
ASF	Alaska SAR Facility
ATC	Air Traffic Control
BCD	Binary Compressed Decimal

CCT	Computer Compatible Tape
CEOS	Committee on Earth Observation Satellites
ESA	European Space Agency
FM	Frequency Modulation
GEC	SAR Ellipsoid Geo-Coded Products.
HDDR	High Density Digital Recorder
HDDT	High Density Digital Tape
IPF	Instrument Processor Facility
MDA	MacDonald Dettweiler Associates
PRF	Pulse Repetition Frequency
PRI	SAR Precision Image Product ***or*** Pulse Repetition Interval (i.e. 1/PRF)
RAW	Formatted Raw Data Product.
RFI	Radar Frequency Interference
SAR	Synthetic Aperture Radar
SHF	SAR Header File
SLC	Single Look Complex Product.
SWST	Sampling Window Start Time
UHF	Universal Header File
UTC	Universal Time Code

2 SEASAT SAR – Background

2.1 SEASAT-A

SEASAT was the first space-based civil EO SAR mission, launched by NASA on June 28th 1978. The mission failed after only 105 days as a consequence of a catastrophic on-board short-circuit but nevertheless managed to acquire data covering 100 million square kilometres (~10,000 standard 100x100 Km scenes) during its 98 days of operation [RD-01]. However the success of the short mission and the quality of some of the EO data acquired was instrumental in demonstrating the utility of space based SAR sensors for EO applications.

SAR data was downlinked by SEASAT to a number of receiving groundstations located in the Northern hemisphere: four North American groundstations (Goldstone (California), Fairbanks (Alaska), Merrit Island (Florida), and Shoe Cove (Newfoundland)) and one European groundstation (Oakhangar, UK).

The SEASAT orbit and acquisition characteristics were similar to those of the subsequent ESA ERS-1/2 EO missions: a retrograde polar orbit at ~800 Km altitude; 23 degree incidence angle; ~100Km swath width (6 degree elevation beamwidth) and comparable range and azimuth resolution (19 MHz chirp bandwidth, ~ 1000+ Hz useable Doppler bandwidth).

SEASAT operated however at L-Band (1.3GHz) in contrast to the ERS C-Band (5.3 GHz) missions.

The ESA SEASAT data archive is derived from reception by the Oakhangar groundstation; it comprises ~ 80 GByte of raw SAR data, with ~350 standard scenes acquired in 32 satellite data takes.

2.2 SEASAT Imagery Redux

There is a resurgence of interest in reprocessing and making historic SEASAT data available to users. This arises in part as a consequence of a general move to make all EO archives from all platforms more user accessible and to harmonise their metadata and status, and in part because of prospective technical research applications, not least analysing changes evolving over the last 35 years by comparison of SEASAT images with e.g. more recent comparable ENVISAT ASAR image data.

Reprocessing the data archive has allowed the SEASAT image products to be generated in formats compatible with current EO systems, as well as generating machine accessible catalogue metadata in a format accessible by current EO databases.

From a technical perspective SAR processing software has also improved materially since the 1980s and the quality of image products (particularly full resolution complex datasets) generated by the SEASAT-IPF is noticeably better than such historic image data that may have been previously processed and archived. The SEASAT-IPF also incorporates a filter to reduce the impact of RFI from coastal, ATC and primary radar systems on the SEASAT data (a ubiquitous problem at L-band) and images.

The Alaska SAR Facility (ASF) have recently reprocessed their North American SEASAT data archive [RD-02]. The ESA European SEASAT archive had previously been reported as unprocessable by the ASF facilities. The cause of this difficulty was that critical metadata (satellite orbit and attitude data) was missing in the header files of the European archive data.

The ESA SEASAT SAR data has however been successfully reprocessed using historic Oakhangar restituted SEASAT orbit and attitude data files, and, aside from cleaning up various technical issues with the

data, the raw data archive has now been rewritten to correctly include orbit and attitude data in the header files, for external interoperability.

3 Rehabilitation of the ESA European SEASAT Data Archive

3.1 Historic SEASAT raw data archive

The downlinked raw data was digitised at the groundstation prior to recording on an HDDR and subsequently transcribed to CCT. The data on the HDDRs was transcribed to CCT in the early 1980s in a format designed by MDA and the data on the CCTs subsequently transferred to disc files at some later date. The original low level SEASAT telemetry data no longer exists and only the secondary disc file archive of MDA-transcribed data is available.

The historic ESA SEASAT raw data archive consists of ~1800 data files; each file is derived from a reel of 1600bpi transcribed CCT containing 4096 echoes. The files are arranged in scene folders corresponding to data frames; the raw data from successive reels is (generally) contiguous within each archived raw scene.

The MDA transcription process was analogous to L0->L1.0 CEOS raw data product formatting, with the low level high rate bit stream processed to generated a formatted data file, with one packed echo and a data header per output record and with additional files generated to contain ephemeris and attitude data and other metadata.

There are a number of problems with the historic data archive stemming from inaccurate azimuth data timing, with timing bias errors of up to several seconds[1]. Each transcribed raw echo has a time stamp embedded in the echo data header; the timestamp evolves consistently with the Pulse Repetition Interval (PRI) (with some material anomalies discussed in section 4) over all the reels spanning any framed raw data product in the historic archive.

A consequence of the timing bias errors is that image data generated from the historic archive has a very poor along track georeference.

A substantial proportion of the data in the historic archive consists of successive frames of data along track that have a degree of data overlap, with the echoes towards the end of a frame duplicated by echoes at the beginning of the subsequent frame along track. Inspection of echoes duplicated in adjacent frames, identified by a bit match of the echo data itself reveals the surprising fact that the timestamps of the echoes frequently differ substantially – the dataset timing biases vary erratically between overlapping frames in the archive. This is not a consequence of bit errors on the embedded clock data and it is clear that by some mechanism MDA introduced timing offsets to the data on a frame by frame basis during the transcription of each frame of raw data.

The data framing of the historic archive is also inaccurate, such that it is not necessarily possible to generate contiguous image data where the raw data frames overlap, because the overlap is frequently smaller than the SAR azimuth footprint.

These problems have been largely successfully resolved and the historic SEASAT raw data archive has been rehabilitated. We discuss the sequence of activities involved below; figure 3-1 gives an overview.

3.2 SEASAT raw data archive translation

The first activity in rehabilitating the SEASAT raw data archive was to concatenate the raw data contained in the ~1800 raw data subfiles into contiguous datasets. This was accomplished in 2 stages.

[1] and in a few instances up to 1 minute.

The first stage was to “cat” the contiguous files corresponding to separate CCT reels within each existing framed raw data scene to generate a single datafile for each of the 351 data frames of the archive.

The second stage was to systematically analyse the raw data of each frame to identify raw data frames that overlapped, and appending the data from such overlapping frames to recover extended contiguous strips of raw data. The 351 raw data frames were thus reduced to 125 strip datasets.

As commented above, the timing information embedded in the header of each data echo proved inconsistent between frames, but it proved readily feasible to concatenate overlapping raw data frames by searching for corresponding echo data records in the region of overlap between frames. The ~70,000 bits of an echo make a very robust synchronisation code and this has allowed the timing of data in each overlapping frame to be rationalised to a common time origin and a contiguous raw data strip to be successfully assembled.

The concatenation of the existing scene based raw data into strips facilitates the georeferencing of the archive as well as making the data in overlap regions accessible as image product.

3.3 SEASAT raw data archive georeferencing

The next stage in rehabilitating the archive was to focus the raw strips of data and to analyse the georeference of the resulting image data, to infer an azimuth timing correction and any sample window start time (SWST) errors.

The majority of the data strips cover some identifiable land or coastal feature. Georeferencing of the 125 data strips was undertaken manually, measuring the difference between feature coordinates obtained from GoogleEarth with their SAR image coordinates, to establish an accurate azimuth timing origin for each data segment and, where relevant, an SWST correction.

Where feasible, georeferencing has been achieved by this means to a reasonable accuracy, of order 50 metres.

3.4 SEASAT raw data archive regeneration

In addition to generating image products the SEASAT-IPF has been designed to generate “cleaned” raw data products in MDA format according to specified acquisition start/stop times, with a SAR Header File (SHF) created and correctly populated with orbit and attitude metadata.

Products and associated metadata have been generated by using the SEASAT-IPF to bulk reprocess the georeferenced archive. Both strip and framed products have been generated, with the strip raw data resegmented into overlapping frames. RAW, SLC, PRI (all in CEOS format) and GEC (GEOTIFF format) products have been created and archived; product specifications can be found in [RD-06].

The SEASAT-IPF RAW data products have been corrected for a number of problems inherent in the source radar data:

- Echo sequencing errors. The source data is prone to echo sequencing errors, with both missing and erroneous pulses. Echo sequencing (discussed further below) has been subjected to careful analysis, and echoes have been inserted or deleted accordingly in the cleaned raw product to maintain azimuth timing integrity.

  It should be noted that any echoes inserted into the dataset to maintain azimuth timing have ***not*** been null-filled – the SEASAT raw data format is 5-bit (0-31) with a bias offset of 15.5, such that a null sample represents a saturating (low) raw data pixel. Any echoes inserted are simply copies of

the previous valid echo; the frame synch field has however been rewritten to record an error status for any such echoes.

- Echo timing field. The echo timing field has been rewritten for each echo, to contain an accurate (precision of the field is 1 msec) timestamp, incorporating the estimated georeferencing timing corrections.

  The echo timing field in the cleaned raw data product uses the accurate PRI, such that the recorded time of echo N is: start_time + (N-1)PRI. The (inaccurate) timing field in the source data is derived from a terrestrial clock, and the cleaned raw data is subtly different in this respect to that held by the North American archives.

- Sample Window Start Time (SWST) field. This is defined, in BCD, in units of the PRI/64. This field has been rewritten to incorporate manually determined SWST corrections, as may be relevant.

Figure 3-1 Overview of ESA SEASAT Raw Data Archive Rehabilitation Procedure

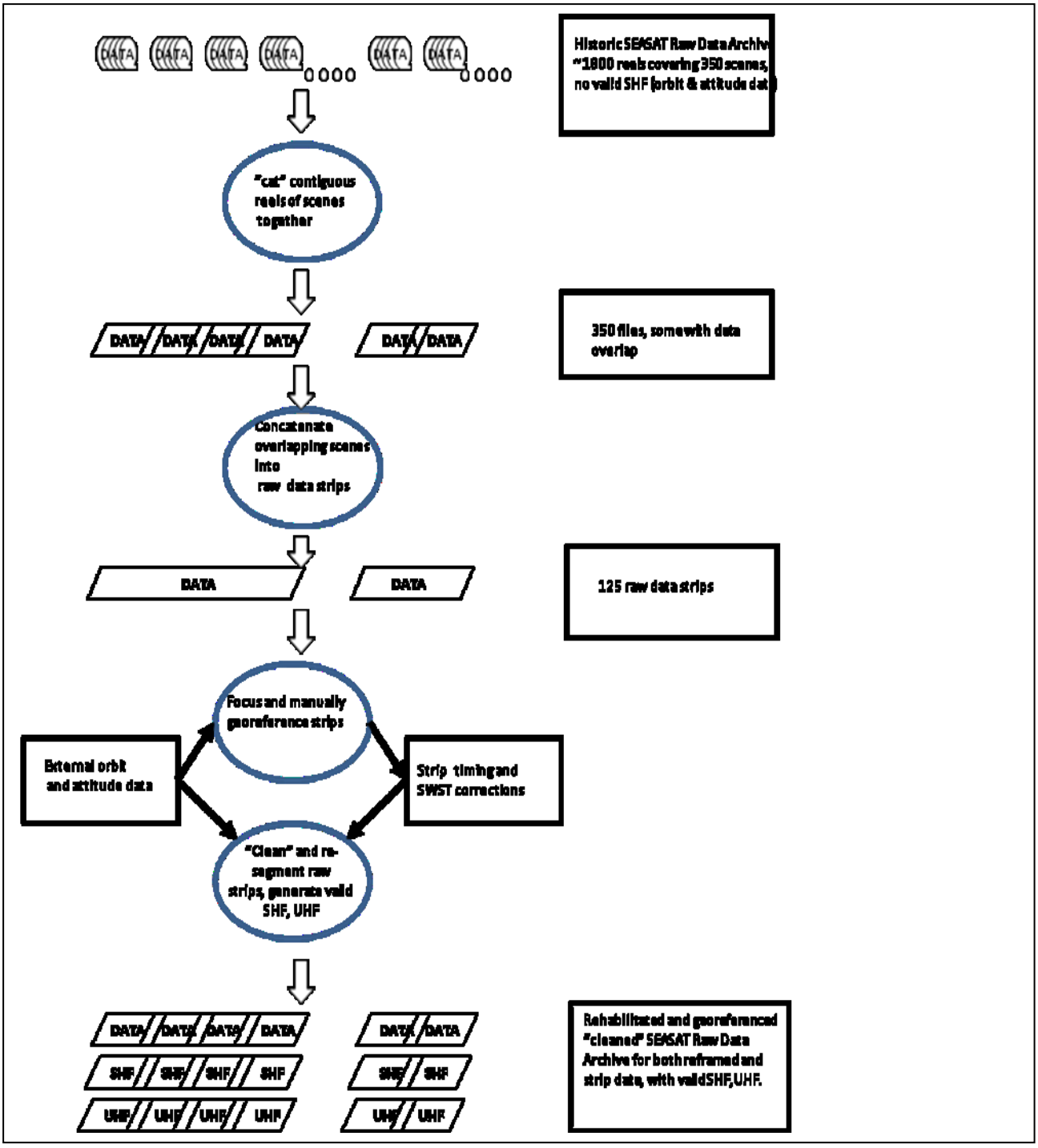

4 SEASAT SAR Processing and Data Issues

4.1 Introduction

In this section we describe some of the key problems associated with the SEASAT raw data that have needed to be addressed in the development of the SEASAT-IPF SAR processor and various residual technical issues.

The topics discussed here are:

- Echo timing characteristics and correcting for echo sequencing errors
- SWST errors
- Range chirp optimisation
- Image radiometry
- RFI and image artefacts
- Extended sequences of missing pulses

4.2 Echo timing and sequencing errors

4.2.1 Introduction

On initial processing of the data we observed a number of problems in the resulting images; several scenes had regions substantially blurred along track, and the image georeference was inconsistent between the start and end in some images, particularly in extended strip images.

These effects are characteristic of echo sequencing errors. Pulse echoes can be lost for example during transcription from HDDT as a consequence of e.g. bit errors corrupting frame synchronisation patterns. For good quality processing it is essential to accurately track pulse timing to maintain a correct azimuth time history. A single dropped/surplus pulse will effectively degrade the azimuth resolution by of order a PRI unit over an extended region of image; with multiple errors the image data quality becomes quite unacceptable at anything other than at a browse-level spatial resolution.

The SEASAT satellite did not embed any echo counter in the downlink telemetry to facilitate monitoring of the integrity of the pulse echo sequence (or, if it did, it was not incorporated into the metadata transcribed by MDA).

A UTC timestamp quantised in integer milliseconds is however embedded in the header of each (MDA transcribed) SEASAT raw data echo record and we attempted to analyse the echo timestamps to locate and correct any echo sequencing errors; in this we have been successful, as discussed below.

The echo timestamp data exhibits two features which make analysis of the echo timing data difficult:

- First, the clock data is noisy – the noise has the characteristic statistics of bit errors – clock errors of e.g. 1,2,4,8, .. 32768 etc msec are equally likely.

- Second, although the clock data has a precision of 1 msec it is apparent that the recorded clock data was updated asynchronously to the PRF and with an (erratic) refresh rate of several msecs.

A further complication is that the recorded clock data does not relate to time on board the satellite, but to a ground based clock and is probably derived from an HDDR timing track.

4.2.2 Echo timestamp characteristics

We analysed the SEASAT clock timing data in terms of the discrepancy λ between the difference in embedded clock time, ΔT, between pulse N and the first echo, with the expected time difference given, in units of PRI, by:

$$\lambda(N) = PRF.\Delta T - (N-1)$$

λ then represents the total number of missing echoes at any point in time. This parameter is real valued because the clock data is not updated synchronously with each echo; typically λ progressively decreases with successive echoes until a timing update is eventually made, when it will revert to an approximately (to within 2 pulses) true value.

Figure 4-1 illustrates the typical behaviour of λ in detail over a sequence of 200 echoes from a SEASAT scene covering Vancouver. The figure illustrates both the asynchronous and erratic clock data updates and also shows timing values corrupted by bit errors – in this instance these corrupted values have been cropped to avoid over-compressing the figure on the vertical axis – the corrupted timing data elements have λ values with large magnitudes.

Figure 4-1 $\lambda(N)$ - Typical Characteristics of the SEASAT Echo Data Timestamp

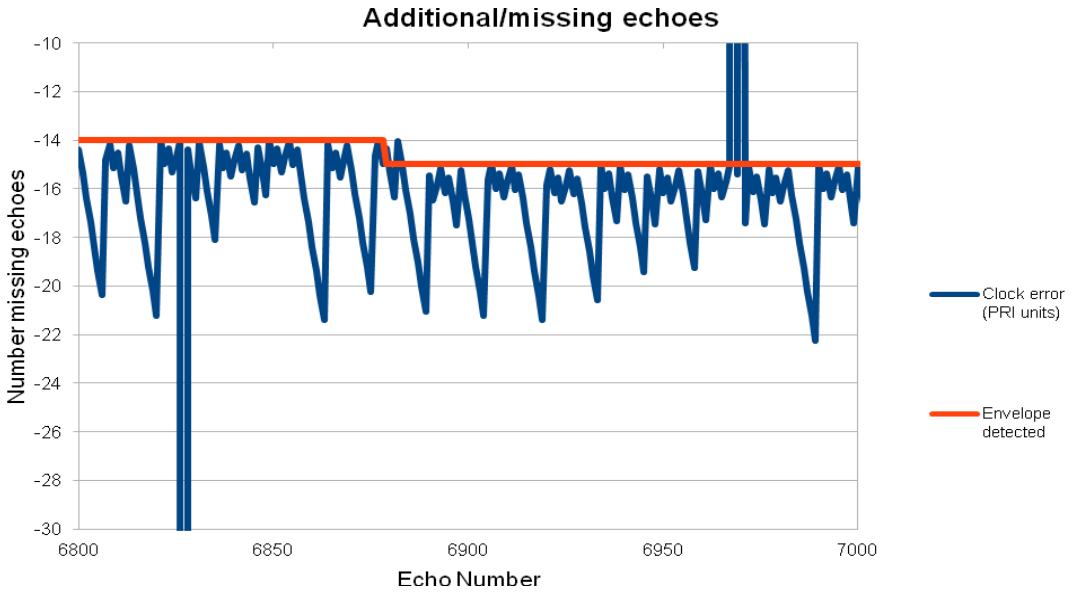

The recorded clock data has a precision of only 1 millisecond corresponding to approximately 2 PRI (the PRF is ~ 1600Hz). However, despite the coarse timing resolution and the erratic clock data updates, a clear step change in λ can be seen in figure 4-1 at around echo 6870, as highlighted by the upper envelope fitted to the data. The sense of the diagram is such that the step change corresponds to an ***insertion*** of a spurious echo into the expected sequence.

Figure 4-2 illustrates the same timing data over a larger set of pulses. With the exception of an event around echo number 8200 corresponding to some missing echoes this timing data indicates a progressive insertion of spurious echoes into this dataset at a rate of around 1 spurious echo per 400 pulses, or around 10 spurious pulses within a SEASAT azimuth correlation length.

In general both missing and additional spurious echoes are identified on many datasets in the archive. The mechanism by which the spurious pulse echoes were inserted is unclear, but their existence is unambiguous. These echo sequencing errors are not unique to the ESA SEASAT archives; the data for figures 4-1 and 4-2 relate to an MDA transcribed dataset on loan from the North American SEASAT archive.

Figure 4-2 SEASAT Echo Data Timing Envelope covering Vancouver Harbour

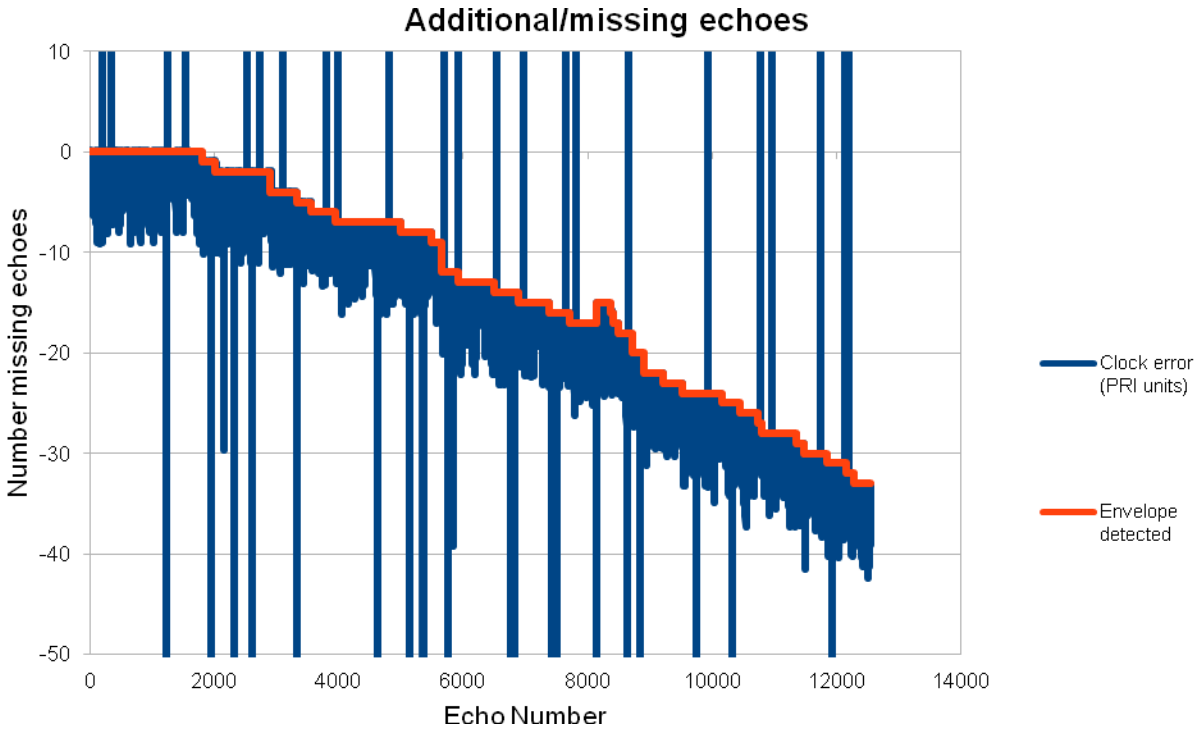

It would be quite wrong to attempt to adjust the dataset to track missing/surplus echoes inferred on the basis of the high frequency variations of the clock error as illustrated in Figure 4-1 – these do not represent any physical truth, other than inaccurate timekeeping. The upper envelope however does illustrate a statistically significant step change in λ. On the hypothesis that the high frequency variations in λ arise because of asynchronous clock data refresh, λ takes a maximum value when the clock refresh is coincidentally

synchronous with an echo, and the upper envelope then approximates an integer number of missing pulses, the true value of λ(N).

Over a large number of echoes the echo timestamp can be seen to drift against the PRI, as evidenced by the envelope of λ(N) drifting from integer values – the average difference in recorded timing values between successive echoes is subtly different from the PRI. It is highly unlikely that this effect is due to some imprecision in the PRF; the PRF, ADC rate, centre transmit frequency etc. were all derived by integer factors from a common stable local oscillator.

Figure 4-3 illustrates the (unwrapped) clock drift measured from mod(envelope(λ(N)),1.0) on a representative dataset, strongly suggesting that the timing reference is derived from a ground based clock. SEASAT downlinked received echoes (in analog form) in real time to a groundstation; the interval between the time of reception of successive pulses is determined by both the PRI and the platform velocity along the downlink line-of-sight. On extended datasets the clock drift can be seen to be only approximately linear, changing with the evolving line-of-sight/orbit geometry.

It is straightforward to estimate the drift rate and to correct λ(N) prior to evaluating the envelope, to derive the true integer values of missing/surplus echoes.

Figure 4-3 Satellite Clock/Ground Clock drift derived from mod(envelope(λ(N)),1.0)

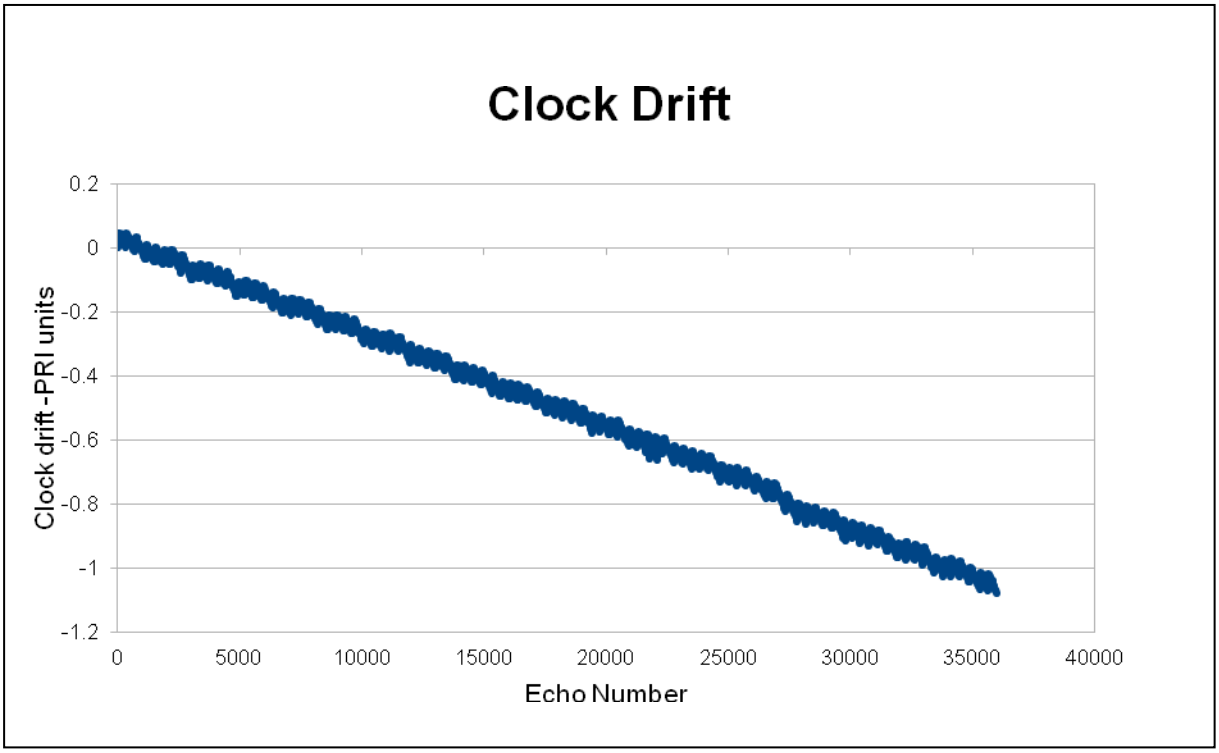

4.2.3 Echo sequence correction

The SEASAT-IPF analyses the echo timing data as described above, correcting the azimuth timing by inserting or deleting echoes into the raw dataset to track the inferred value of λ(N). Although residual localised errors will occur in the estimation of the location of dropped/surplus pulses these have no systemic effect – a correct azimuth timing history is recovered for e.g. >99% of the dataset.

We note that the ASF also undertake a careful analysis of the echo timing data as discussed in [RD-02], although it is unclear quite how the information is supplied to their processor. Some analogous and effective compensation is however clearly also undertaken by the ASF; figure 4-9 further below shows a geocoded detail of both the SEASAT-IPF and ASF GEC images derived from the same raw dataset used for generating figure 4-4 - the ASF image is reasonably well focused at a PRI resolution.

Figures 4-4 to 4-6 illustrate the dramatic effect on image quality of correcting the azimuth timing. Figure 4-4 is the image data corresponding to the echo timing sequence shown in figure 4-2 above.

These figures are PRI-style (~25m resolution, 12.5m pixels) SEASAT images generated before and after analysing the clock timing data and correcting for dropped/surplus echoes. In the figures the “before” image is at the left of the figure and the “after” image at the right.

In general we have now obtained crisply focused images for all data in the ESA SEASAT archive.

Figure 4-4 Vancouver Harbour detail before and after correction for λ*(N)*

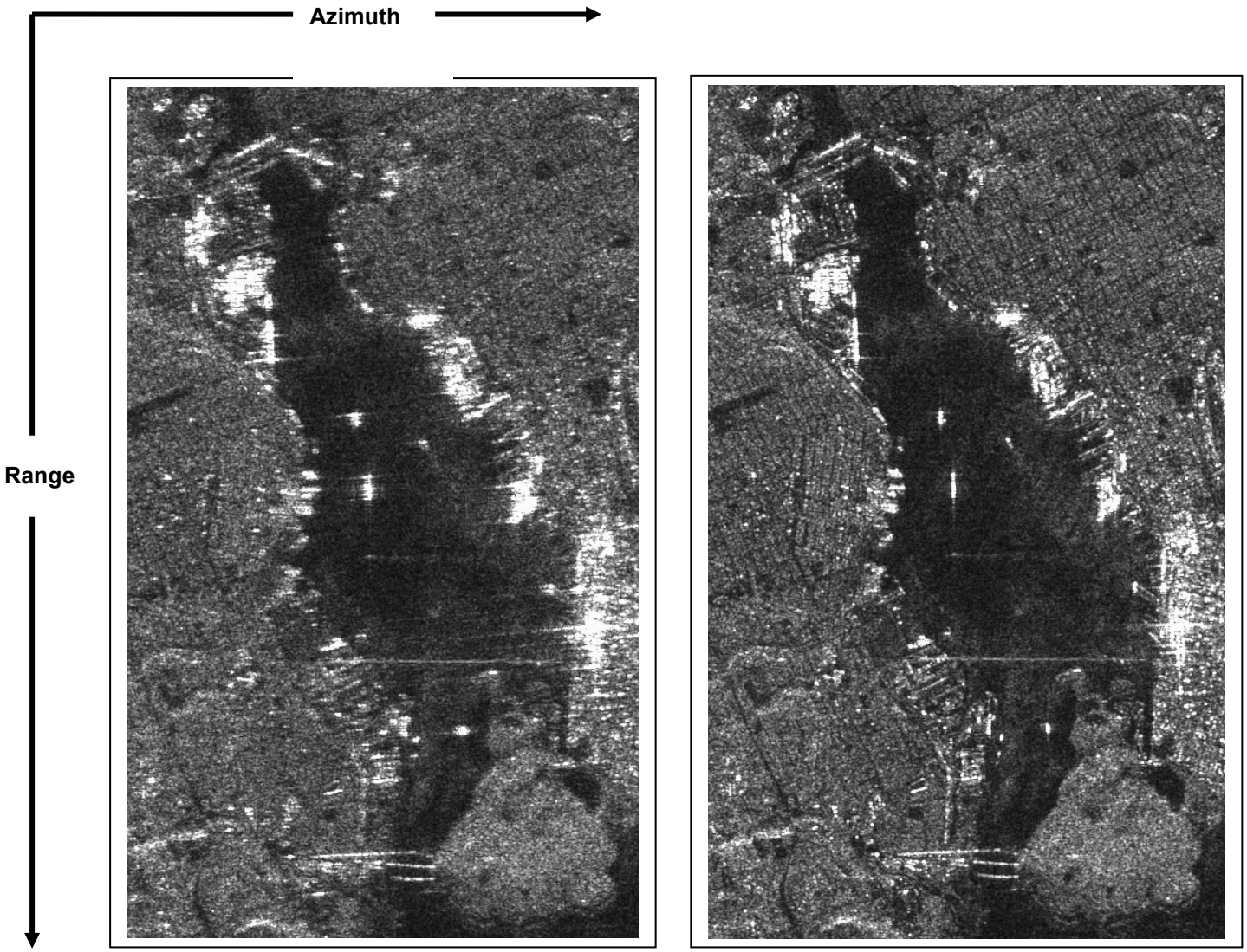

Figure 4-5 Goldstone scene detail before and after correction for $\lambda(N)$

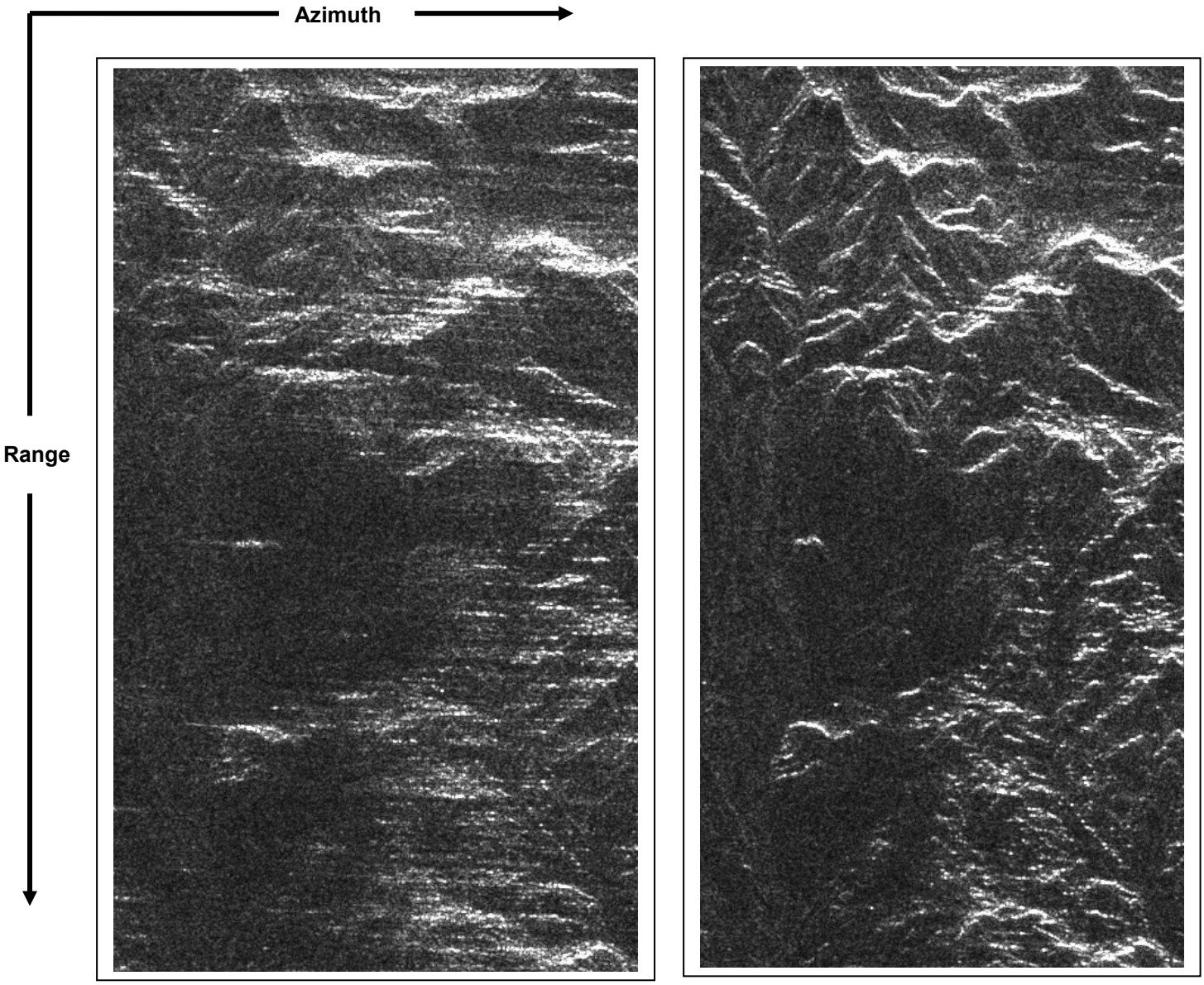

Figure 4-6 Vancouver Island detail before and after correction for $\lambda(N)$

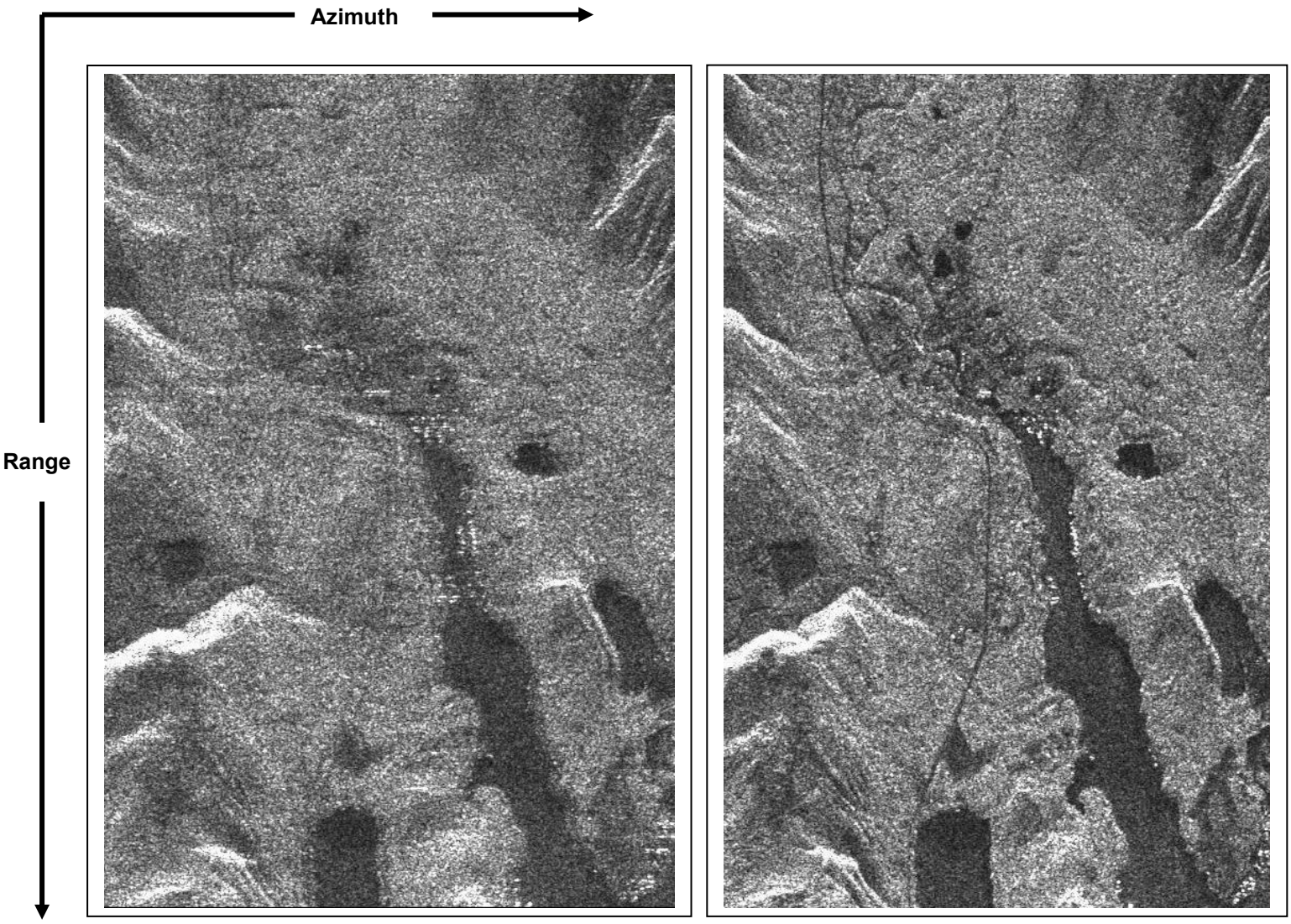

4.3 Sampling Window Start Time (SWST) errors

The SWST determines the range origin of the echo data – it is a platform parameter adjusted to ensure that the receive window is roughly centred around the return from antenna boresight and may change at any time during an acquisition. For SEASAT it is quantised in units of 1/64 of a PRI, approximately equivalent to 1.44Km in 1-way slant range. This important parameter is reported on a pulse by pulse basis in each transcribed raw echo data header.

In general the reported SWST accurately matches the data. However on one orbit (762) in the ESA archive the reported SWST remains constant but clearly changes over the orbit, from inspection of the data and the image range georeference between data acquired initially early in the orbit over the southern Mediterranean and subsequently over Greenland.

Errors in reporting the SWST are readily identified by large range georeferencing errors and are confirmed by image azimuth misfocus arising from the related mismatched azimuth compression. It is not known why SEASAT's reporting of SWST codes should be erratic, but is presumably a consequence of some optional control mode for the satellite. This phenomenon is well known and is also documented by the ASF.

The SEASAT-IPF allows an optional timing corrections file to be associated with any SEASAT dataset to define both an azimuth timing correction and an integer SWST correction. After correcting for integer SWST errors the range georeferencing errors for all acquisition segments of orbit 762 are consistent with the other datasets (of the order of 50 metres).

We have identified (unsurprisingly) that there is an unrecorded SWST adjustment by 1 unit within one of the orbit 762 acquisition segments, resulting in image blurring over the transition region and a range georeference error in the subsequent image data along track. The location of the SWST change was identified by visual correlation of streaks from bright scatterers in the range compressed data (see figure 4-7 below) and a software utility created to correct the SWST code in the headers of echoes subsequent to the unreported SWST change. No artefacts from bright points are now discernible in the image of the corrected data and the image georeference is now uniformly consistent.

Figure 4-7 *Detail of range compressed data before and after correction of raw data for an unreported SWST change*

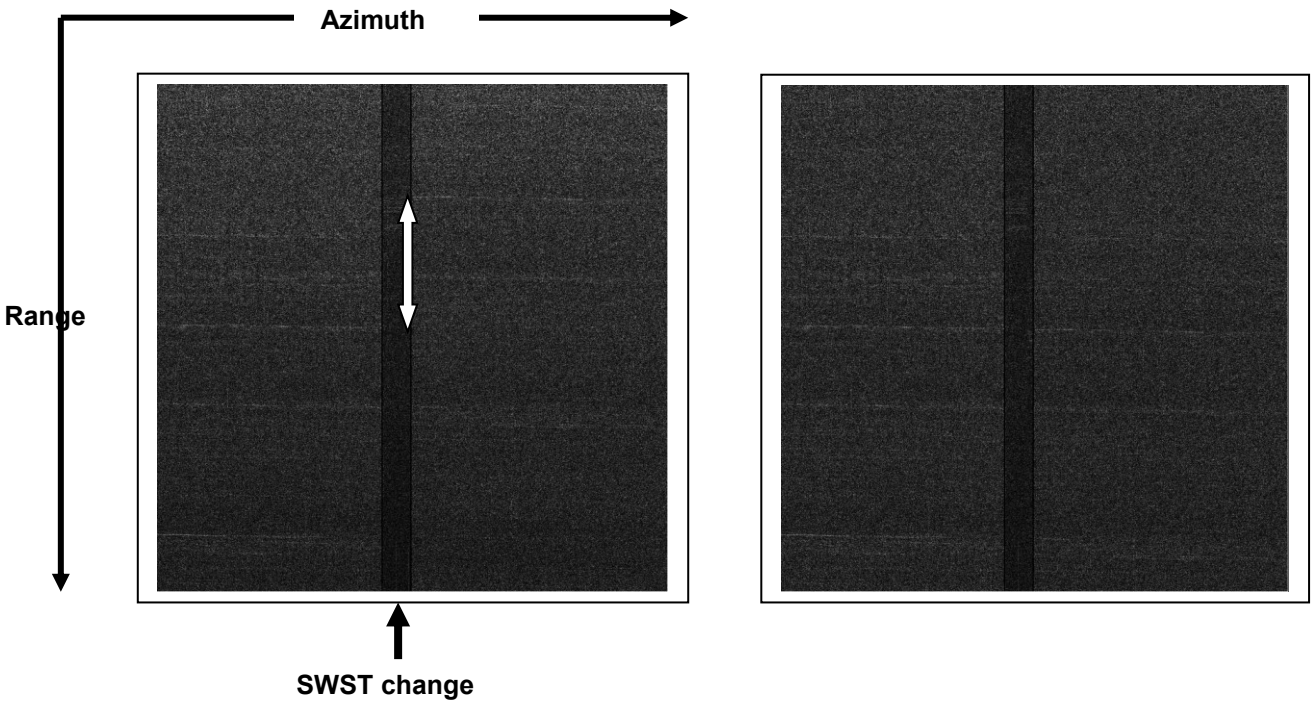

In figure 4-7 the null space around the SWST change is some feature of the satellite operation; we surmise that at around the time of an SWST change it ceases transmission, such that the received data is just thermal noise for a few echoes.

We have not noticed any SWST issues with the other ESA archive datasets, but this remains a QA issue for any images that might possibly be generated from other externally supplied SEASAT raw datasets.

Valid SWST changes have been observed occurring in other ESA SEASAT archive datasets.

4.4 Range chirp optimisation

The documented parameters available to us for the SEASAT pulse chirp are approximate values and we have refined them empirically.

Trigger bias

The trigger bias delay has been estimated from the measured range georeferencing errors, averaged over the ESA archive.

We estimate the trigger bias as : **7.41** microseconds.

The SEASAT swath is such that it has a rank of 9 (there are 9 PRI between pulse transmission and echo reception.

The time offset to first echo sample is thus given by: **(9/PRF) + SWST_CODE/(64*PRF) – 7.41.10^{-6}**seconds.

Chirp FM rate

The chirp FM rate has been estimated by numerically maximising image contrast. We parameterise the FM rate in terms of nominal chirp bandwidth and nominal chirp duration.

The SEASAT chirp is an upswept FM glide with a bandwidth of: **19077225.0** Hz and a duration of **33.9277** microseconds, an accurate estimate of the FM rate is: 19077225.0/33.9277 = +**562290.54725195** MHz/sec.

Chirp non-linearities

The SEASAT chirp is uniform in amplitude.

There is however a small non-linearity in the FM rate. This has the effect of distorting the range sidelobe levels, with an elevated first sidelobe at far range.

A correction for this has been estimated empirically. We characterise the cubic term in the (video) frequency domain:

If f is the single sideband video frequency and f_{ADC} is the ADC sampling rate, then the cubic phase correction is approximately given, for the baseband signal, by:

$-2\pi*0.015*(4*f / f_{ADC})^3$ **for** $-f_{ADC}/4<f<+f_{ADC}/4$ radians (i.e. -0.015 cycles cubic phase error at the edges of the (single sideband) sampling bandwidth).

Figures 4-8 and 4-9 below illustrate the range impulse response with and without the cubic chirp correction. These figures were generated from an SLC (1200 Hz, unweighted) image over an oil refinery, interpolated by a factor of 8; the (further interpolated) range profile corresponds to that of the scatterer within the highlighted box centred on the cursor cross-hairs.

The cylindrical oil storage tanks provide useful point-like scattering responses.

In figure 4-8 the first sidelobes are asymmetrical, with one elevated by ~3 dB and one reduced by ~3dB, but are reasonably balanced in figure 4-9. Overall the characteristics of the impulse responses exhibited in figure 4-9 agree well with expected values and there is no evidence of any processor-related focus degradation.

Figure 4-8 Interpolated image and impulse response range profile (linear amplitude) without chirp cubic phase correction

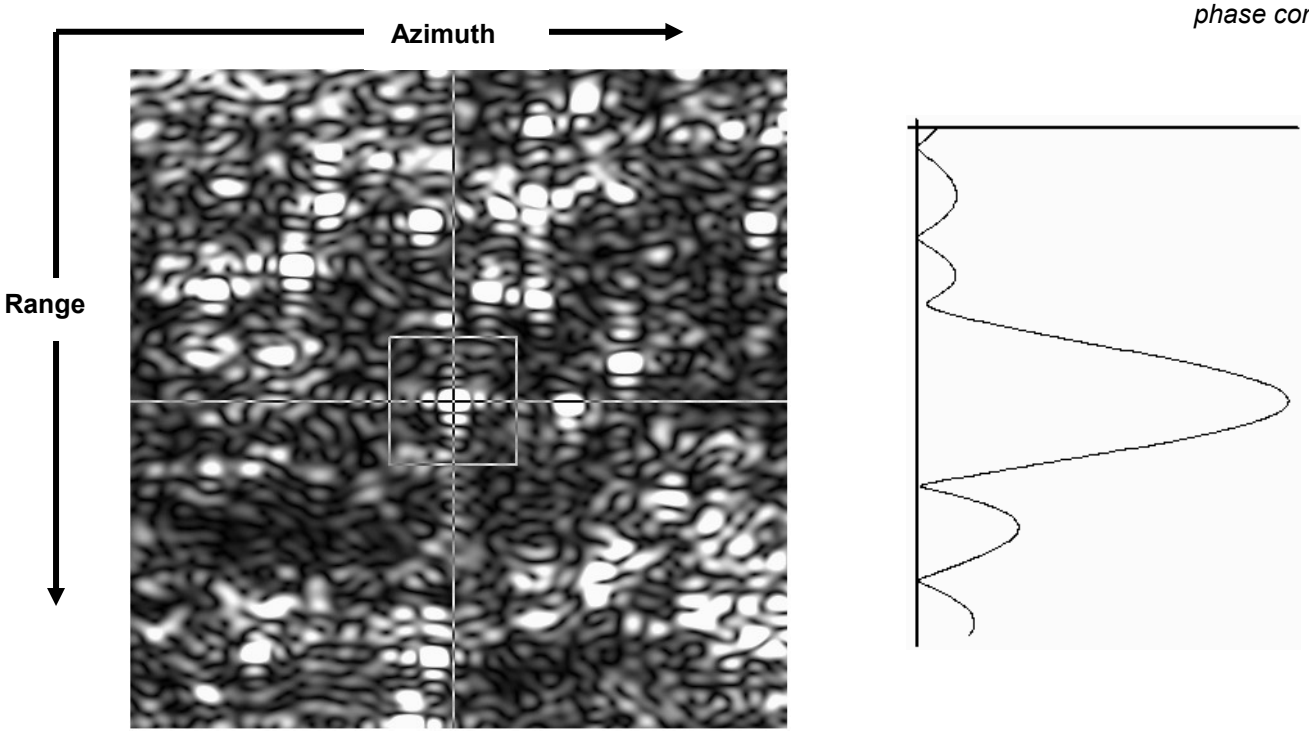

Figure 4-9 Interpolated image and impulse response range profile (linear amplitude) with chirp cubic phase correction

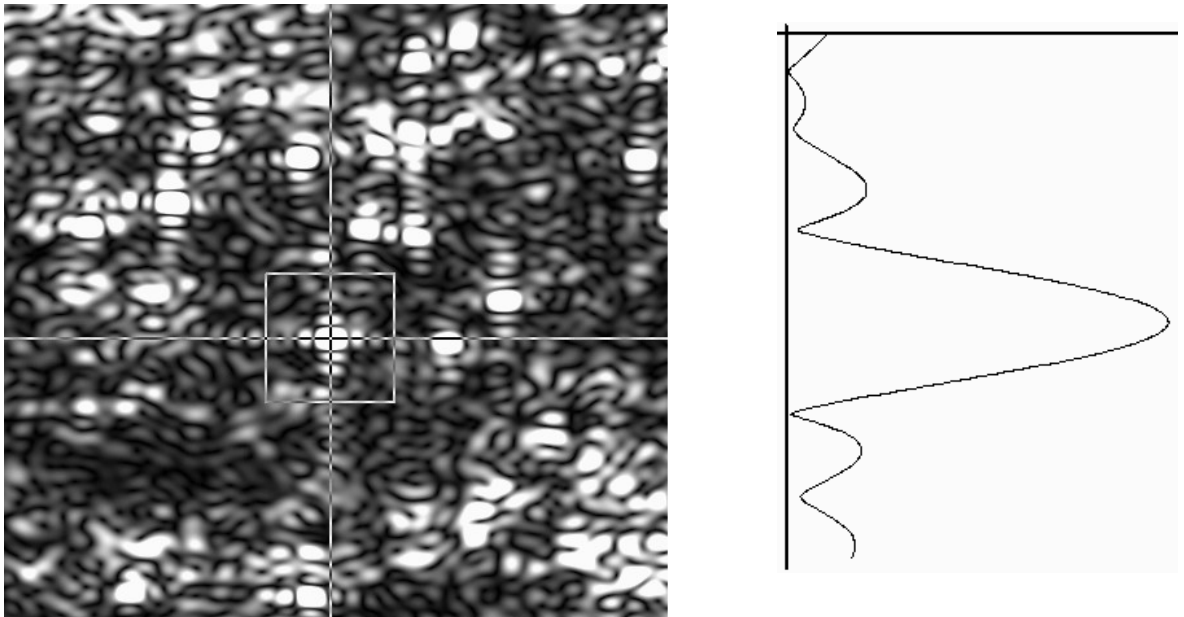

4.5 Image radiometry

There remain some limitations concerning the quality of the image radiometry generated by the SEASAT-IPF.

4.5.1 Calibration

The ESA SEASAT raw data archive is a secondary archive of MDA transcribed data; the original low-level SEASAT telemetry files no longer exist. The telemetry information provided in the MDA echo record headers is extremely limited, and in particular there are no details on any platform gain settings. As a consequence the radiometric calibration of the processed data is uncertain; it has all been processed on the assumption that the platform gain settings were constant over the mission. We do not currently know whether this was the case or not. SEASAT was also equipped with an AGC although there is no evidence of its operation in any of the acquisitions covered by the ESA archive.

4.5.2 STC

SEASAT operated using Sensitivity Time Control (STC). This imposes a range-dependent gain on received echoes prior to download to reduce the dynamic range of the echo data. The STC pattern represents an approximation to the net signal gain contributions from spreading loss and the antenna pattern.

The SEASAT-IPF applies an inverse STC pattern to the raw data, subsequently applying radiometric corrections for the elevation antenna pattern and spreading loss. The inverse STC pattern applied is however only approximate; currently we have no accurate STC engineering data, and the pattern used is a simple “V” shape covering 9dB from the centre of the pattern to its edges. This is based on a comment made in RD-03.

In general the cross-swath radiometric equalisation is reasonable, but on some scenes there is a suspicion that the STC pattern is slightly mislocated. The SEASAT-IPF assumes that the pattern applied has an origin that adjusts automatically with the SWST; this is not necessarily the case – in JERS-1 for example the SWST and STC origins could be adjusted independently. Unfortunately any data concerning the STC origin is not represented in the transcribed echo headers.

It may be possible to improve the radiometric quality if relevant SEASAT satellite engineering documents can be found that define an accurate STC pattern and which might clarify any mission control options for setting the origin of the applied STC pattern.

4.6 RFI and other image artefacts

4.6.1 RFI

Radio Frequency Interference (RFI) from ground based radar systems is a significant issue at L-band and the SEASAT-IPF incorporates a reasonably effective technique to eliminate both CW and narrow-band RFI with minimal impact on image quality and radiometry.

The effects of uncompensated RFI on SAR image products are dependent on the characteristics of the contamination and can result in either prominent image artefacts or a substantial increase in the image noise floor.

Figure 4-10 shows a detail of a SEASAT scene (processed to GEC) over Vancouver by the ASF and the same scene processed by the SEASAT-IPF.

The prominent streak on the ASF image is almost certainly due to a narrow-band high power transponder associated with Vancouver airport. The image streak is focussed in range because the transponder returns a proportion of the transmit chirp bandwidth, but its return is not accurately phase-locked to the received SEASAT chirp and is consequently defocused along track (the direction of the streak, in these geocoded images).

The SEASAT-IPF is reasonably successful at eliminating this RFI contamination.

Figure 4-10 RFI contamination over Vancouver (Detail from ASF and SEASAT-IPF GEC images)

ASF image **SEASAT-IPF image**

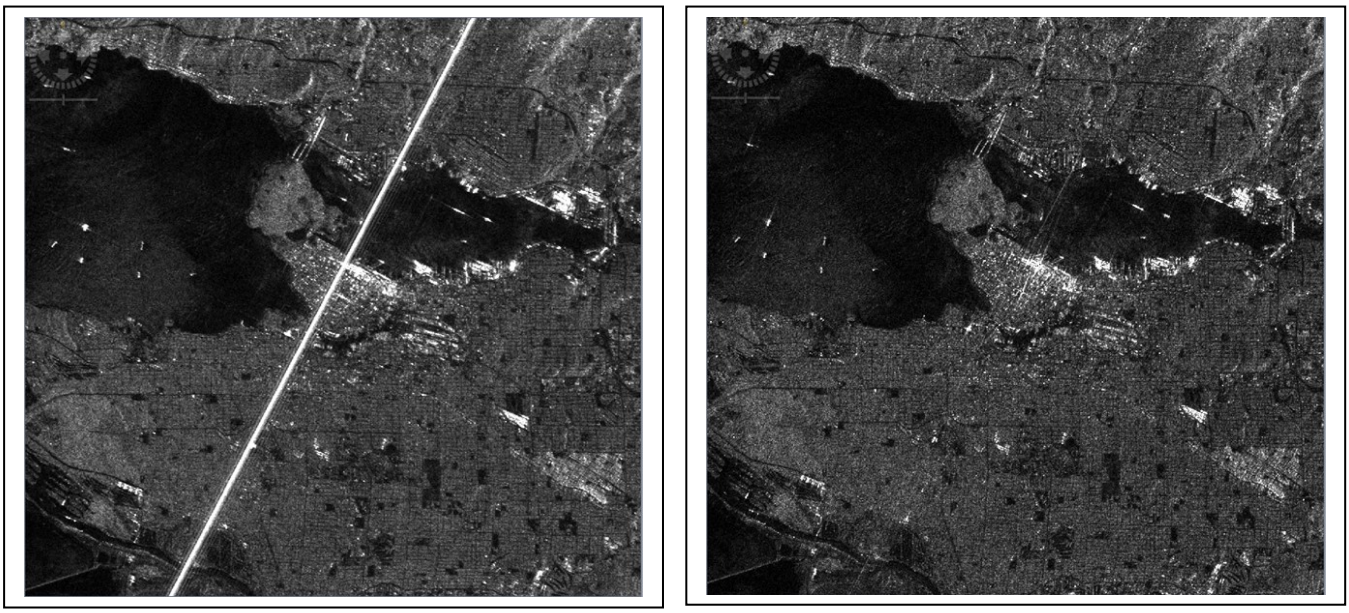

The current SEASAT-IPF RFI filter operates in the range frequency domain and identifies and eliminates statistically significant spikes or runs. The filter is not however currently effective against all types of RFI. Figure 4-11 below illustrates a detail from a SEASAT-IPF image exhibiting the effects of strong RFI that escapes the current strategy.

On investigation, in this case the RFI looks as though it comes from a range-Doppler radar system. The SEASAT-IPF spectral filtering is ineffective because the RFI materially covers the SEASAT chirp bandwidth. The RFI is clearly evident as streaks (in range) in the range compressed data. In this instance the RFI chirp is partially compressed leading to short but very bright streaks scattered in a semi-periodic fashion (the PRF of the RFI radar is asynchronous with the SEASAT PRF) across the range compressed data. Although the energy in these streaks is then dispersed in azimuth by azimuth compression they still contain sufficient energy to generate the “barcode” effect visible against the relatively low rcs image of the sea surface.

An appropriate strategy for eliminating this type of RFI would be a suitable statistical filter operating on the range compressed data in the time domain. The power variations in range in the range compressed data are

highly correlated along track and it should be readily feasible to identify and eliminate the (very) small number of pixels with high RFI power with a low false rejection rate and a good detection performance.

This may be implemented as a future refinement, although we note that artefacts such as exhibited by figure 4-11 appear on only a few of the ESA SEASAT archive datasets.

Figure 4-11 RFI in a SEASAT_IPF image

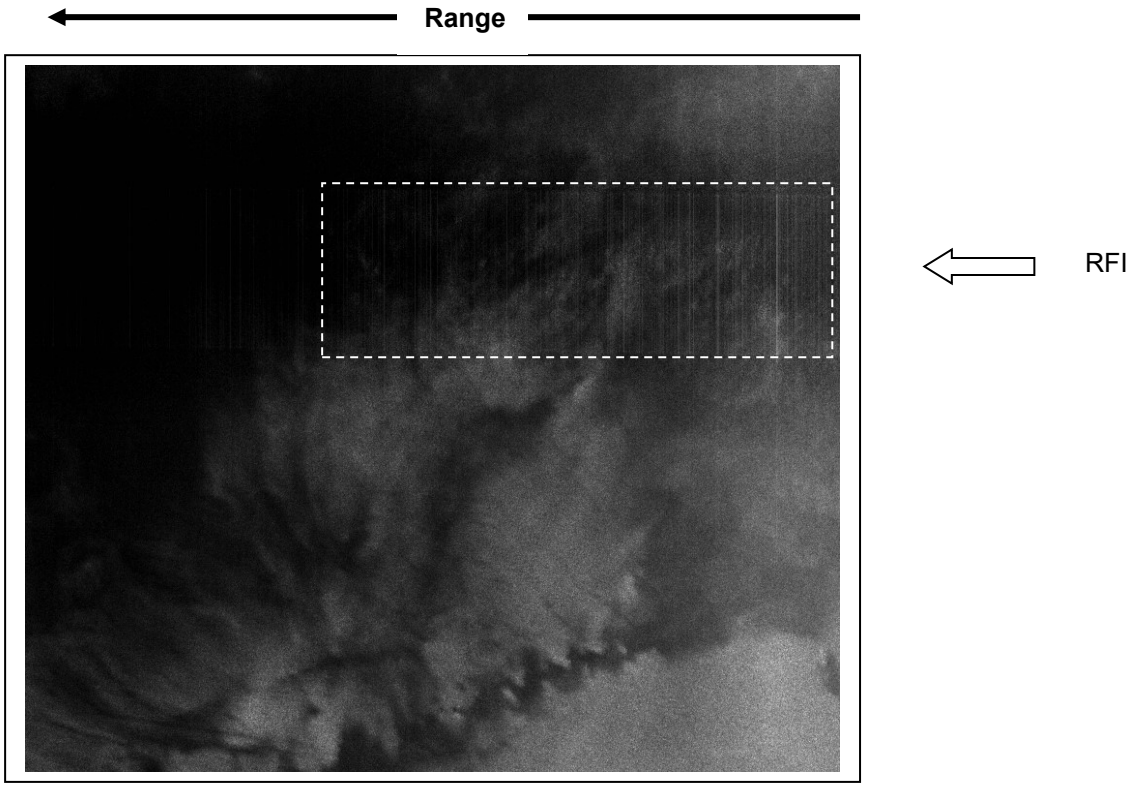

4.6.2 SEASAT calibration signals

The SEASAT platform incorporated a feature to inject “calibration” signals into the received echo data.

The nature of the signal injection was to insert a copy of the transmitted chirp into a series of a few hundred echoes at some range offset, then to repeat the process at a range incremented by a few hundred range samples.

The purpose of this was presumably to allow some direct measurements to be made of gains in the receiver and downlink electronics, and/or possibly to provide a mechanism to extract a reference copy of the transmitted chirp waveform. The SEASAT mission failed before it entered its planned operational phase and this feature was activated on a few acquisitions held in the ESA SEASAT archive, which exhibit associated image artefacts. Figure 4-12 shows a detail of such a scene containing such artefacts.

The compressed calibration signals are very clear in the range compressed data and it would be readily feasible to filter them out.

This may be implemented as a future refinement, although we note that artefacts such as exhibited by figure 4-12 appear on only a few of the ESA SEASAT archive datasets.

Figure 4-12 Image detail illustrating artefacts arising from injected calibration signals.

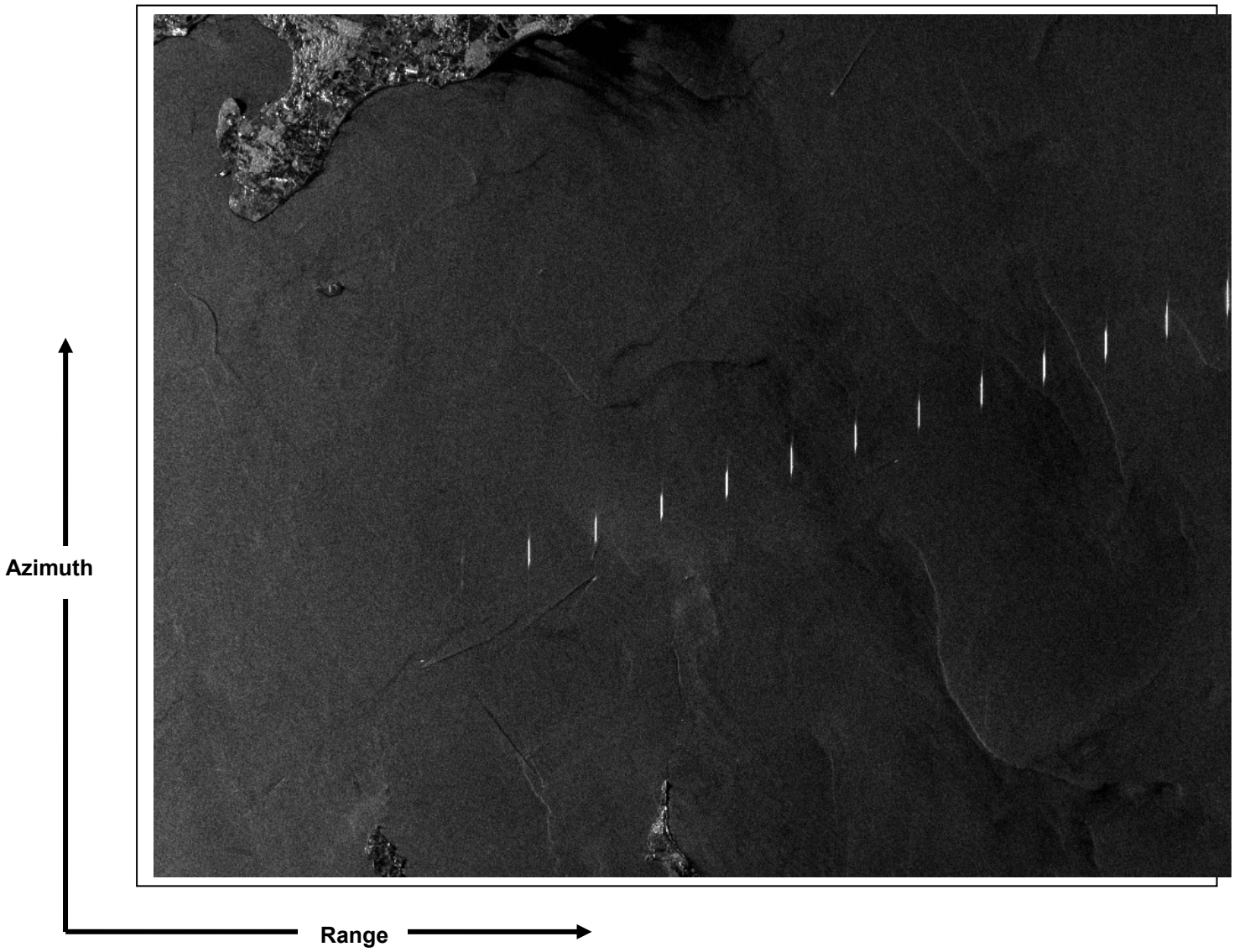

4.7 Extended sequences of missing pulses

As discussed in section 4-1, in some datasets a few echoes are sporadically missing from the transcribed raw data, probably as a consequence of bit errors in the frame synchronisation codes, but these have an insignificant impact on image quality provided the azimuth timing sequence is corrected.

Of much greater significance, some historic archived datasets are missing extended sequences of echoes. In some instances a file corresponding to a complete reel (4096 echoes) is empty, with just a “warning” message. Such missing data sequences presumably date to when the secondary CCT archive data was transferred to disk files and arose due to physical degradation in storage of the transcribed data tapes.

We have adopted a policy of inserting null data to fill any such gaps to avoid further fragmenting the image archive, with the consequence that some scenes exhibit dark bands, with a gradual transition to valid image data at the band edges. The image georeferencing quality is however unaffected by such data loss.

Figure 4-13 below illustrates such a scene.

The ESA archive metadata flags the quality of such scenes as “degraded”.

Figure 4-13 Dataset missing 2 CCT “reels” of data